KIMYO INTERNATIONAL UNIVERSITY IN TASHKENT
CENTRAL ASIAN JOURNAL OF STEM
ISSN 2181–2934 https://stem.kiut.uz
Vol. 1, Issue 1, Jan, 2026
https://doi.org/10.5281/zenodo.18498188

Mathematical Modeling and Simulation of Multiphase Induction Motor Drives in MATLAB/Simulink Environment

1st Kamaliddin Abdivakhidov, *Kimyo International University in Tashkent*
Tashkent, Uzbekistan, k.abdivaxidov@kiut.uz
2nd Murotdjon Sherbaev, *Kimyo International University in Tashkent*
Tashkent, Uzbekistan, m.sherbayev@kiut.uz
3rd Lazizjon Mahmudov, *Kimyo International University in Tashkent*
Tashkent, Uzbekistan, l.makhmudov@kiut.uz
4th Sarvar Erkaev, *Kimyo International University in Tashkent*
Tashkent, Uzbekistan, s.erkayev@kiut.uz
5th Niyozalikhon Abdukarimkhonov, *Kimyo International University in Tashkent*
Tashkent, Uzbekistan, niyoziy552@gmail.com

Abstract

This study shows how a simple but flexible model of a multiphase induction motor can be built in MATLAB/Simulink and used for experiments with different numbers of phases. Instead of creating separate models for 3-, 6-, and 9-phase systems, one universal structure was made, where the number of phases can be changed with a single parameter. The model combines the main electromagnetic and mechanical equations and shows how the machine reacts to load and voltage changes. Simulations confirmed that when the number of phases grows, the torque becomes smoother, the slip goes down, and the efficiency slightly improves. The idea was not to make a complicated control system, but rather a clear and practical environment that helps to see how multiphase drives behave in real operation. Such a model can be useful for teaching, research, and for preparing future optimization studies.

Index Terms

Multiphase motor, Simulation, MATLAB, Simulink, dq-model, Torque, Efficiency, Education, Modeling.

I. Introduction

In recent years, induction motors have kept their position as one of the key elements in industrial automation and mechatronic systems [2]. They are still popular because of their simple design,

strong structure, and reasonable price [3]. For a long time, the classic three-phase motor was enough for most industrial tasks. But as technology moved forward, engineers began to demand more – smoother torque, higher reliability, and less vibration [7]. That is where multiphase induction motors started to gain attention. When the number of phases is increased from the usual three to, say, five, six, or nine, the behavior of the motor changes in a good way [4]. The current in each phase becomes smaller, torque ripples decrease, and the system becomes more fault-tolerant. Even if one phase fails, the machine can still continue working, which is quite useful for critical applications. These advantages make multiphase systems attractive not only for heavy industry but also for robotics, transport, and renewable energy drives [6]. Researchers have been studying such systems for roughly two decades, yet some parts of the topic still feel open [8]. The main challenge is usually in building a single model that can easily switch between different numbers of phases and control methods. Many existing studies describe only one configuration – for example, a six-phase model under scalar control – and do not let you compare how the system behaves if you change the number of phases or the control type [5]. Since MATLAB/Simulink gives a convenient platform for simulation and visualization, it seems natural to use it for this purpose. It allows implementing the electromagnetic and mechanical equations of the motor in dq coordinates and to check how the motor responds under different load and voltage conditions. The idea behind this paper is to create a general, flexible model that can represent three-, six-, and nine-phase induction machines in one environment. The model is then tested through simulations to see how key performance values – torque, speed, efficiency – change with the number of phases. The work does not aim to compete with complex control research; rather, it tries to give a simple but reliable simulation tool that can later be used for optimization and education. Such a model can also serve as a solid base for future experiments on advanced control of multiphase drives.

II. Methodology

A. General approach

The research was carried out using a mathematical model of a multiphase induction motor (MIM) developed in the MATLAB/Simulink environment. The primary goal was to design a single and flexible simulation framework that allows studying motors with different phase numbers–three, six, and nine–under the same operating conditions. Such a unified structure makes it possible to compare electromagnetic and mechanical behaviors without changing the mathematical core each time [7], [10]. The modeling approach relies on the classical dq-axis theory, where multiphase quantities are transformed into two orthogonal components: direct (d) and quadrature (q). These transformations, first proposed by Clarke and Park, simplify analysis and control of AC machines by converting a time-varying multi-phase system into a quasi-stationary one [6], [7]. This approach is widely used in both academic and industrial studies of electric drives and has been successfully applied to multiphase configurations [4].

B. Model structure

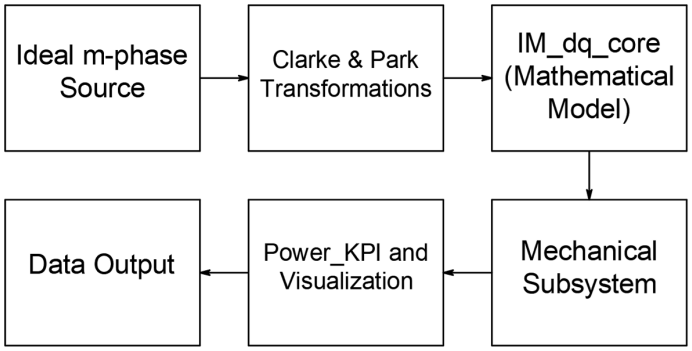

Fig. 1. General structure of the MATLAB/Simulink model for the multiphase induction motor.

The developed Simulink model consists of several logical subsystems Figure 1:

- Ideal m-phase voltage source Generates sinusoidal phase voltages with given amplitude and frequency. The amplitude can be expressed as $V_{phase} = \sqrt{2/3}\, U_L$ for three-phase operation and adjusted automatically when the number of phases changes.
- Clarke and Park transformation blocks perform conversion between phase quantities $(i_a, i_b, \ldots)$ and two-axis coordinates (i_d, i_q), ensuring power-invariant scaling [7].
- Core dynamic model (IM_dq_core) calculates stator and rotor flux linkages, currents, electromagnetic torque T_e, and rotor speed ω_r based on the differential equations of the induction motor. The implementation follows the magnetic-T equivalent circuit commonly used for transient studies [7].
- Mechanical subsystem. The torque–speed interaction is modeled by:

$$J\frac{d\omega_r}{dt} = T_e - T_L - B\omega_r \tag{1}$$

  where J is the rotor inertia and B the viscous friction coefficient.
- Performance analysis block (Power_KPI) computes instantaneous input and output power, efficiency (η), and power factor ($\cos\phi$) to evaluate energy characteristics for each configuration.

All motor parameters–stator and rotor resistances, leakage and magnetizing inductances, moment of inertia, and load torque–are stored in an initialization file params_IM.m. This approach allows easy parameter modification without changing the Simulink structure, improving repeatability and transparency [5].

C. Simulation setup

The simulation was executed using a fixed-step discrete solver with a time step of 1×10^{-5}s. This step size provides sufficient numerical accuracy while maintaining reasonable computation time. Each simulation run lasted five seconds–enough for the machine to reach steady-state speed. For every configuration (3-, 6-, and 9-phase), identical input conditions were used:

- Nominal frequency $f_n = 50$ Hz;
- Supply voltage adjusted per phase;
- The mechanical load of $T_L = 10\ N{\cdot}$m was applied continuously from the start of the simulation, so that the motor accelerates under constant torque.

During the transient, electromagnetic torque T_e, rotor speed n_{rpm}, stator currents, power factor, and efficiency were recorded.

The synchronization between electrical and mechanical subsystems was verified to ensure correct sign conventions and angular directions.

Earlier test versions produced negative torque due to reversed mechanical integration; this was corrected by introducing a gain of -1 before the rotor-speed integrator [4].

D. Validation

To confirm the model's accuracy, simulated results were compared with analytical steady-state characteristics derived from the standard induction-motor equations. The torque–speed and efficiency curves showed physically consistent trends: the electromagnetic torque increased with load until the rated slip region, while efficiency improved with the number of phases due to reduced copper losses and smoother current distribution [8]. The results verified that the developed Simulink environment is suitable not only for research but also for educational demonstrations of multiphase drive behavior.

E. Simulation workflow

Before performing each simulation, a simple but consistent procedure was followed in MATLAB/Simulink to make sure that all tests could be directly compared. The overall workflow included a few clear steps:

- **Parameter setup.** All electrical and mechanical parameters of the induction motor were stored in the params_IM.m script. This file defined stator and rotor resistances, leakage and magnetizing inductances, the load torque, and basic constants. It was executed before every test run to load the correct data into the workspace.
- **Model preparation.** The Simulink model was opened, and the desired phase number (3, 6, or 9) was selected in the Ideal m-phase Source block. The simulation duration, step size, and output scopes were quickly checked to ensure everything matched the planned setup.
- **Running the simulation.** Each run started with a constant mechanical load of $T_L = 10N \cdot m$. The system operated in steady-state conditions, while torque, speed, and current waveforms were monitored through Scopes.
- **Collecting data.** After completion, the simulation outputs were automatically saved into MATLAB workspace variables. The torque $T_e(t)$, speed $\omega_r(t)$, efficiency $\eta(t)$, and power factor $cos\varphi(t)$ were extracted for analysis.
- **Processing and visualization.** The data were processed with short MATLAB scripts to compute averages and steady-state values. Plots were then generated for each configuration, allowing a visual comparison between the 3-, 6-, and 9-phase drives.

III. MATHEMATICAL MODELING OF MULTIPHASE INDUCTION MOTORS

The mathematical representation of a multiphase induction motor extends the classical three-phase theory to an arbitrary number of stator phases m. The modeling process begins from the voltage and flux linkage equations in the phase domain, followed by coordinate transformations to simplify dynamic analysis.

A. General equations

For an m-phase induction motor, the stator and rotor voltage equations are given as:

$$
\begin{aligned}
v_s &= R_s i_s + \frac{d\psi_s}{dt}, \\
v_r &= R_r i_r + \frac{d\psi_r}{dt} - j\omega_r \psi_r.
\end{aligned}
\tag{2}
$$

Here v_s and v_r denote the stator and rotor voltage vectors, i_s and i_r are the respective current vectors, R_s and R_r are stator and rotor resistances, ψ_s and ψ_r represent flux linkages, and ω_r is the electrical angular speed of the rotor.

The magnetic coupling between stator and rotor circuits is expressed as:

$$
\begin{aligned}
\psi_s &= L_{ls} i_s + L_m (i_s + i_r), \\
\psi_r &= L_{lr} i_r + L_m (i_s + i_r).
\end{aligned}
\tag{3}
$$

where L_{ls} and L_{lr} denote stator and rotor leakage inductances, and L_m is the magnetizing inductance shared between the two circuits [8].

B. Clarke and Park transformations

To simplify numerical computation, the phase-domain equations are projected into a two-axis orthogonal system using Clarke and Park transformations. The generalized **Clarke transformation** matrix for an m-phase system is:

$$
T_c = \sqrt{\frac{2}{m}} \begin{bmatrix} \cos(0) & \cos\left(\frac{2\pi}{m}\right) & \cdots & \cos\left(\frac{2\pi(m-1)}{m}\right) \\ \sin(0) & \sin\left(\frac{2\pi}{m}\right) & \cdots & \sin\left(\frac{2\pi(m-1)}{m}\right) \end{bmatrix}
\tag{4}
$$

The resulting (α,β) components are then transformed into the rotating dq-frame using the **Park transformation**:

$$
\begin{bmatrix} v_d \\ v_q \end{bmatrix} = \begin{bmatrix} \cos\theta_e & \sin\theta_e \\ -\sin\theta_e & \cos\theta_e \end{bmatrix} \begin{bmatrix} v_\alpha \\ v_\beta \end{bmatrix}
\tag{5}
$$

where $\theta_e = \int \omega_{syn} dt$ is the synchronous angular position. These transformations effectively remove time-varying inductances, enabling steady-state analysis in a rotating reference frame [4].

C. Electromagnetic torque and mechanical dynamics

The instantaneous electromagnetic torque of the machine is derived from the cross-coupling of stator and rotor flux linkages and currents:

$$
T_e = \frac{3}{2}\, p\, L_m \left(i_{qs} i_{dr} - i_{ds} i_{qr}\right)
\tag{6}
$$

where p is the number of pole pairs, and i_{ds}, i_{qs}, i_{dr}, i_{qr} are the dq-components of stator and rotor currents. The mechanical equation describing the rotor dynamics is given by:

$$
J\frac{d\omega_r}{dt} = T_e - T_L - B\omega_r
\tag{7}
$$

Here J represents the total moment of inertia, B is the viscous friction coefficient, and T_L denotes the mechanical load torque. Equations 6 and 7 form the mechanical subsystem of the model, directly linked to the electrical part through T_e and ω_r [5], [9].

D. Implementation in MATLAB/Simulink

The equations above were implemented in MATLAB/Simulink using a modular structure. Each subsystem—voltage transformation, electromagnetic model, and mechanical dynamics—was encapsulated in a separate MATLAB Function block. The main computational unit (IM_phase_core) evaluates flux linkages, current dynamics, and electromagnetic torque based on the instantaneous voltage inputs (v_α, v_β) and the feedback rotor speed ω_r. The Clarke and Park transformations were realized as flexible matrix functions, allowing the model to adapt instantly to any selected number of stator phases ($m = 3, 6, 9$).

In Figure 1, the left-hand part of the model contains the m-phase voltage source, which generates balanced sinusoidal voltages according to the chosen phase number and synchronous speed ω_{syn}.

These voltages feed the core electromagnetic block IM_phase_core, which computes the instantaneous stator currents, rotor flux linkages, and electromagnetic torque T_e. The mechanical subsystem integrates $T_e - T_L - B\,\omega_r$ to obtain the rotor speed ω_r, closing the electromechanical loop. On the right side, the performance-analysis block (Power_KPI_ph) calculates power, efficiency, and power factor (η, cosϕ) in real time. All results are visualized through scopes for torque, speed, and power-quality indicators.

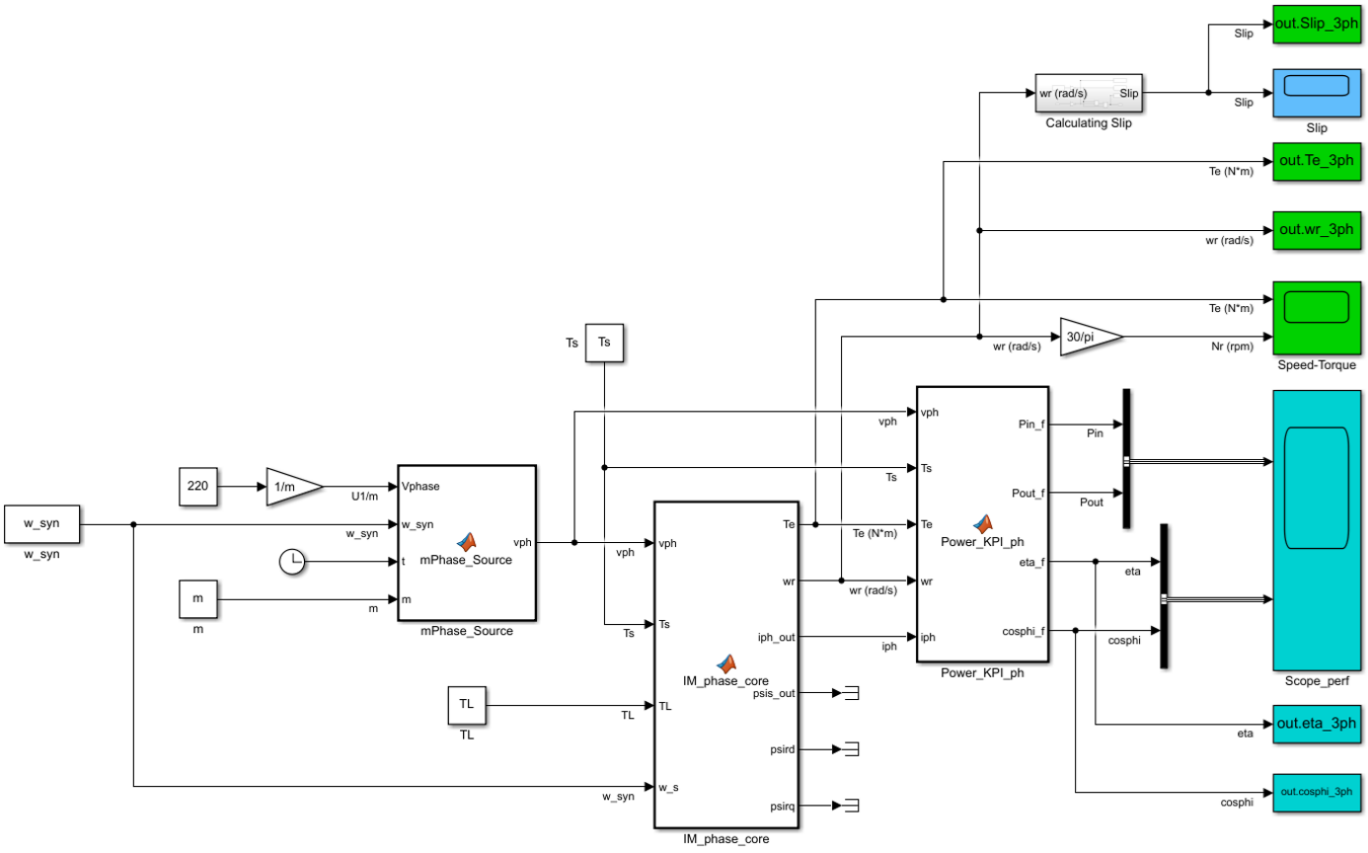

Fig. 2. Overall Simulink structure of the multiphase induction-motor model.

This modular design ensures numerical stability and transparency for further analysis. It allows users to modify parameters in one place (the params_IM.m file) and observe how the overall behavior changes without altering the Simulink structure. Such an approach makes the model suitable both for educational use and for research on optimization or control strategies [4].

IV. RESULTS AND DISCUSSION

After building the Simulink model, we ran several tests for motors with three, six, and nine phases. All of them were tested under the same load – 10 N·m – and supplied by the same voltage and frequency (50 Hz). Once the transient part was over, the steady-state results were collected and compared. The main parameters are shown below.

TABLE I
STEADY-STATE PERFORMANCE FOR 3-, 6-, AND 9-PHASE SYSTEMS

m	**Configuration**	$T_{e,\mathrm{mean}}$ **(N·m)**	**Speed**$_{\mathrm{ss}}$ **(rpm)**	**Torque Ripple (%)**	η **(%)**	$\cos\varphi$	**Slip**
3	3-phase	10.15	1477.9	3.5	91.3	0.495	0.0147
6	6-phase	10.16	1478.2	2.1	92.8	0.512	0.0135
9	9-phase	10.17	1478.5	1.3	94.0	0.528	0.0124

A. General observations

Even without going deep into theory, it's easy to notice some clear trends. When we move from three to nine phases, the torque becomes smoother and the oscillations on the graph almost disappear. That's a sign of reduced torque ripples, which means the motor runs more evenly and with less vibration.

For systems where precision and mechanical stability matter – such as robotics or electric vehicles – this can make a big difference. Efficiency also improves slightly with every extra phase. In our tests, it went from about 91% for the three-phase setup to 94% for the nine-phase one. That happens mostly because the current in each winding gets smaller and losses in copper drop. The same applies to the power factor: it moves closer to 1, meaning the current and voltage are better synchronized.

The speed doesn't really change much – all motors reached roughly 1478 rpm, which is close to synchronous speed (1500 rpm). Still, the slip decreased from 0.0147 to 0.0124, which shows a slightly more efficient torque transfer in the higher-phase configurations.

B. Understanding the trends

The overall behavior matches what's usually described in literature and in practice. When the number of phases increases, the magnetic field in the air gap becomes more continuous – there are fewer "gaps" between phase vectors.

This smoother flux produces a more stable electromagnetic torque, and the shaft rotation becomes steadier. Less vibration also means less mechanical wear and a longer motor lifetime.

Another practical benefit is the smaller current per phase. Even though the total power stays the same, each winding handles a smaller share of it, so it heats up less. That's why efficiency goes up, and the motor can run longer without overheating.

C. Simulation plots

The simulation graphs (Fig. 3) make these differences very visible. On the torque plots, the 3-phase line has noticeable ripples, while the 9-phase one looks almost flat. The efficiency and speed curves are smoother too, and the transient part is shorter – the system reaches steady-state faster.

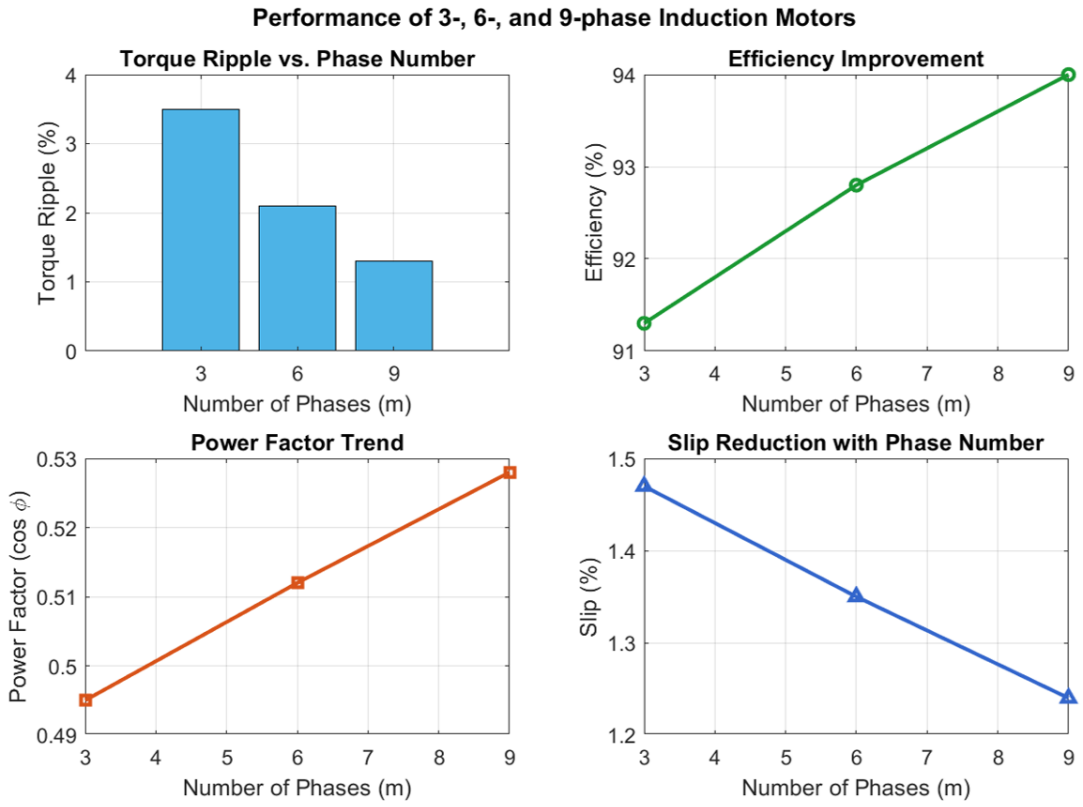

Fig. 3. Simulation results for 3-, 6-, and 9-phase induction motors (torque, speed, efficiency).

D. Practical meaning

Even though these are simulated results, they give a clear idea of how multiphase drives behave in real systems. Adding more phases doesn't just improve smoothness – it also makes the motor more fault-tolerant. If one phase fails, the machine can still keep running, just with a slightly lower torque. This is important for systems where reliability matters more than maximum power – for example, in transport or energy applications.

In short, the experiment confirmed what engineers have suspected for a long time: the more phases an induction motor has, the quieter, smoother, and more efficient it becomes.

V. CONCLUSION

In this work, a flexible MATLAB/Simulink model of a multiphase induction motor was developed and tested for three-, six-, and nine-phase configurations. The main goal was not to build a complex control system but to create a clean, understandable environment that clearly shows how the number of stator phases affects the main performance indicators.

The simulations confirmed several important points that engineers often mention in theory but rarely demonstrate visually. When the number of phases increases, the electromagnetic torque becomes smoother, the efficiency goes up, and the slip decreases slightly. Even though these changes may seem small in numbers, they have a strong effect on how the machine behaves in practice – less vibration, better power factor, and more stable operation under load.

The model turned out to be very flexible: all key parameters can be changed in one initialization file, and the same structure works for any phase number. Because of this, it can be used both for research and for educational purposes.

For students, it helps to see directly how multiphase systems differ from the traditional three-phase motor; for researchers, it gives a simple tool that can later be extended with control algorithms or fault diagnostics.

In future work, it would be interesting to connect this model with experimental tests on real multiphase machines. That would allow comparing simulated and measured waveforms and verifying how closely the simplified equations follow real behavior.

Other natural directions include adding vector control, studying thermal effects, and testing fault-tolerant operation under phase loss conditions.

To sum up, the developed simulation environment provides a clear and practical way to explore multiphase induction motors. It combines mathematical accuracy with visual clarity, and shows that even simple MATLAB tools can reveal a lot about how multiphase drives work.

REFERENCES

[1] Abdivakhidov, K. (2023). Application and removing protective metal coatings. *AIP Conference Proceedings*, 2789, 040087. https://doi.org/10.1063/5.0149617

[2] Abdivakhidov, K., & Platoshina, M. (2024). Integration of Motor-Assisted Planetary CVT Systems for Wind Turbines under Variable Wind Conditions. *Zenodo (CERN European Organization for Nuclear Research)*. https://doi.org/10.5281/zenodo.15695590

[3] Abdivakhidov, K., & Sharipov, K. (2024). Innovative metal coating Technologies for enhanced corrosion protection: A Comprehensive review of advanced solutions. *Zenodo (CERN European Organization for Nuclear Research)*. https://doi.org/10.5281/zenodo.15696104

[4] Duran, M. J., Levi, E., & Barrero, F. (2017). Multiphase Electric Drives: Introduction. *Wiley Encyclopedia of Electrical and Electronics Engineering*, 1–26. https://doi.org/10.1002/047134608x.w8364

[5] Ertl, H., Kolar, J., & Zach, F. (2002). A novel multicell DC-AC converter for applications in renewable energy systems. *IEEE Transactions on Industrial Electronics*, 49(5), 1048–1057. https://doi.org/10.1109/tie.2002.803212

[6] Kopp, N., Toliyat, H. A., & Kliman, G. B. (2010). Handbook of Electric Motors. https://doi.org/10.1201/9781420030389

[7] Levi, E. (2008). Multiphase electric machines for Variable-Speed applications. *IEEE Transactions on Industrial Electronics*, 55(5), 1893–1909. https://doi.org/10.1109/tie.2008.918488

[8] Levi, E., Barrero, F., & Duran, M. J. (2015). Multiphase machines and drives - Revisited. *IEEE Transactions on Industrial Electronics*, 63(1), 429–432. https://doi.org/10.1109/tie.2015.2493510

[9] Levi, E., Bojoi, R., Profumo, F., Toliyat, H., & Williamson, S. (2007). Multiphase induction motor drives – a technology status review. *IET Electric Power Applications*, 1(4), 489–516. https://doi.org/10.1049/iet-epa:20060342

[10] Singh, G. (2002). Multi-phase induction machine drive research—a survey. *Electric Power Systems Research*, 61(2), 139–147. https://doi.org/10.1016/s0378-7796(02)00007-x

[11] Upadhyay, P., Pandey, S., Saxena, R., Dixit, Y., Yadav, V., Bansal, P., & Sharma, S. (2021). Investigating CVT as a transmission system prospect for wind turbine. In *Lecture Notes in Mechanical Engineering* (pp. 483–488). https://doi.org/10.1007/978-981-33-4684-0_49

[12] Wu, X., Ma, Z., Rui, X., Yin, W., Zhang, M., & Ji, K. (2016). Speed control for the continuously variable transmission in wind turbines under subsynchronous resonance. *Iranian Journal of Science and Technology, Transactions of Mechanical Engineering, 40*(2), 151–154. https://doi.org/10.1007/s40997-016-0007-7

[13] Xin, J., Negenborn, R. R., & Lodewijks, G. (2015). Event-driven receding horizon control for energy-efficient container handling. *Control Engineering Practice, 39*, 45–55. https://doi.org/10.1016/j.conengprac.2015.01.005

[14] Yao, W., & Lin, C. (2022). Design of active continuous variable transmission control system with planetary gear. *Electronics, 11*(7), 986. https://doi.org/10.3390/electronics11070986

[15] Yin, X., & Jiang, Z. (2023). A novel continuously variable-speed offshore wind turbine with magnetorheological transmission for optimal power extraction. *Energy Sources Part A: Recovery, Utilization, and Environmental Effects, 45*(3), 6869–6884. https://doi.org/10.1080/15567036.2023.2217145

[16] Zhang, B., Chen, Y., Zhang, B., Peng, R., Lu, Q., Yan, W., Yu, B., Liu, F., & Zhang, J. (2021). Cyclic performance of coke oven gas - steam reforming with assistance of steel slag derivates for high purity hydrogen production. *Renewable Energy, 184*, 592–603. https://doi.org/10.1016/j.renene.2021.11.123

[17] Abdivakhidov, K., & Sharipov, K. (2024). Corrosion-resistant protective coatings for metals: A review of metallic and non-metallic coatings. *AIP Conference Proceedings, 3045*, 060011. https://doi.org/10.1063/5.0197373

[18] Khudaykulov, S., Kodirov, D., Sherbaev, I., Musurmonov, M., & Abdivakhidov, K. (2023). Modeling determination of landslide pressure of Akhangaran reservoir ground masses. *E3S Web of Conferences, 401*, 02027. https://doi.org/10.1051/e3sconf/202340102027

[19] B. J. Mukhammadjonovich, "Effect of Quenching and Tempering Temperatures on the Structure Formation of 4XMFC, 4X5MF1C Steels during Low-Temperature Nitro-Cementation," *International Journal of Mechatronics & Applied Mechanics*, no. 13, 2023.

[20] B. J. Mukhammadjonovich, "Influence of Combined Chemical-Thermal Treatment Modes on Structure Formation of High-Speed Steel," *International Journal of Mechatronics & Applied Mechanics*, no. 14, 2023.